Proceedings of the 9th U.S. National and 10th Canadian Conference on Earthquake Engineering
Compte Rendu de la 9ième Conférence Nationale Américaine et
10ième Conférence Canadienne de Génie Parasismique
July 25-29, 2010, Toronto, Ontario, Canada • Paper No 146

VISCOUS DAMPER LIMIT STATES AND COLLAPSE ANALYSIS OF STEEL FRAME BUILDINGS WITH DAMPERS

H. K. Miyamoto[1], A. S. J. Gilani[2], and A. Wada[3]

ABSTRACT

A hybrid design of sizing members for strength limits and using fluid viscous dampers to control drift is a robust and cost-effective solution for low to high rise structures. Dampers are used to provide energy dissipation to the system and to protect steel members and connections. The dampers are sized per recommendations provided in ASCE/SEI 7 for new structures. The damping devices are designed and constructed to satisfy the maximum considered earthquake (MCE) response. Laboratory production tests are conducted to verify that the dampers meet the constitutive relations assumed in analysis. Performance in past earthquakes has shown that structures designed in such method perform well in earthquakes. However, to date, no detailed investigation has been undertaken to assess the collapse performance of structures with viscous dampers. In typical applications, the engineers analyze structures with dampers without consideration for the damper limit states and terminate their investigations at the MCE level. However, the limit states of viscous dampers have a significant effect on the response of the building to which they are attached to. To address this issue, a refined model of viscous dampers has been developed based on the force-displacement-velocity constitutive relations of the damper components and incorporating the damper limit states. This model incorporates displacement and force limit states. Simulations were conducted to check the limit state activation for the model. Experimental data were then used to verify the accuracy of such limit states. The refined damper model was then implemented in analytical models of steel archetypes and incremental dynamic analysis was conducted to determine the collapse behavior of steel moment frames with viscous dampers.

Introduction

Viscous dampers were originally developed as shock absorbers for the defense and aerospace industries. Figure 1 presents photographs of a viscous damper. Viscous dampers have been used extensively for seismic application for both new and retrofit construction (Miyamoto and Gilani 2008). During seismic events, the devices are activated and the seismic input energy is converted to the heat energy and is thus dissipated. Subsequent to installation, the

[1]President, Miyamoto International, Inc. Sacramento, CA, 95691
[2] Structural Specialist, Miyamoto International, Inc. Sacramento, CA, 95691
[3] Professor, Department of Structural Engineering, Tokyo Institute of Technology

dampers will not require maintenance (Taylor 2007) and have been shown to possess stable and dependable properties for design earthquakes. However, to date the response of structures with viscous dampers have not been studied. Results from an on-going research dealing with such cases are presented in this paper.

Figure 1. Viscous dampers used for design of a new building in California

Development of a Refined Model for Viscous Dampers

Viscous dampers consist of a cylinder and a stainless steel piston. The cylinder is filled with an incompressible silicone fluid. The damper is activated by the flow of silicone fluid between chambers at opposite ends of the unit, through small orifices. Figure 2 shows the damper cross section. In most applications, the dampers are modeled as simple Maxwell model of Figure 3. The viscous damper itself is modeled as a dashpot in series with the elastic driver brace member. Such model is adequate for most design applications, but is not sufficiently refined for collapse evaluation. In particular, force and displacement limit states are not accounted for.

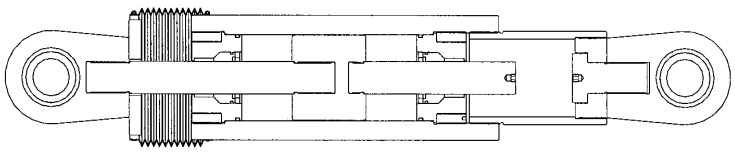

Figure 2. Viscous damper cross section.

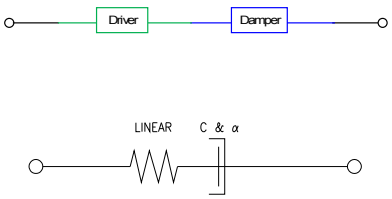

Figure 3. Maxwell representation.

The limit states of viscous dampers are governed by the following criteria:

- When the piston motion reaches its available stroke, the dampers bottoms out. This is the stroke limit and results in transition from viscous damper to a steel brace with stiffness equal to that of the cylinder wall.

- Once the piston undercut fractures in tension or the driver brace buckles, the damper fails and is no longer effective.
- The orifice limit state is reached at high velocities. However, this limit state does not significantly alter the damper response. Such limit state results in change in the damper exponent (α).

Figure 4 presents the refined model for viscous dampers. This model is developed to incorporate the pertinent limit states and consists of five components. The refined model consists of the following components.

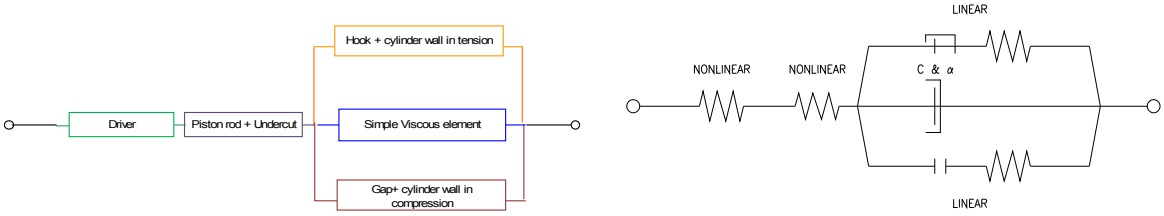

Figure 4. Refined model for viscous dampers.

- The driver brace used to attach the damper to the gusset plates at the beam-to-column connection is modeled as a nonlinear spring.
- The piston rod (including the piston undercut) is modeled as a nonlinear spring. The piston undercut is the machined down section between the end of the piston and the start of the piston male threaded part. In tension, the undercut section of the piston can yield and then fracture. The undercut area is approximately 80% of the full piston area. The piston ultimate strength is only 10% above yield. Hence, fracture follows yielding rapidly; see Figure 5.
- Dashpot is used to model the viscous component.
- Gap element and linear springs are used to model the limit state when the piston retraction equals the stroke. The elastic stiffness is dependent on the damper construction and its cylinder properties.
- Hook elements and linear springs are used to model the limit state when the piston extension reaches the damper stroke. The stiffness is the same as for the gap element.

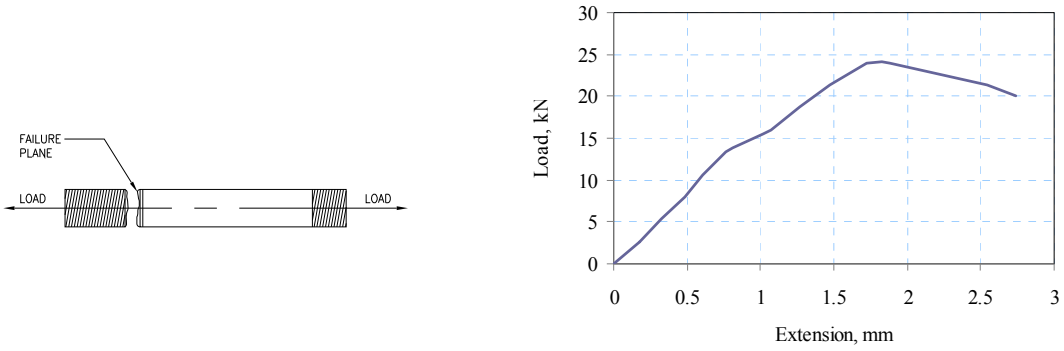

Figure 5. Piston undercut section and test data.

Analytical Studies

To illustrate the response of the refined model and illustrate its capability to capture all the limit states, simulations were conducted. The damper was modeled in program OpenSees (PEER 2009) using the refined model. All analysis was conducted using a sinusoidal displacement input function. The damper used in simulation is the 700-kN unit and has a constitutive relation (force in kN and velocity in mm/sec) of Eq. 1

$$F = 88\,\mathrm{sgn}(v)|v|^{0.3} \tag{1}$$

Force Limit State of Piston Fracture

This simulation was conducted to investigate the damper response for the limit state of piston undercut fracture. The stroke was artificially set to be large enough to ensure that the damper did not bottom out in compression. The response is shown in Figure 6. Note that the force transmitted by the cylinder walls is zero since the damper has not bottomed out. Once the piston undercut reaches its tensile capacity, the damper element is automatically removed from the simulation and the forces drop to zero.

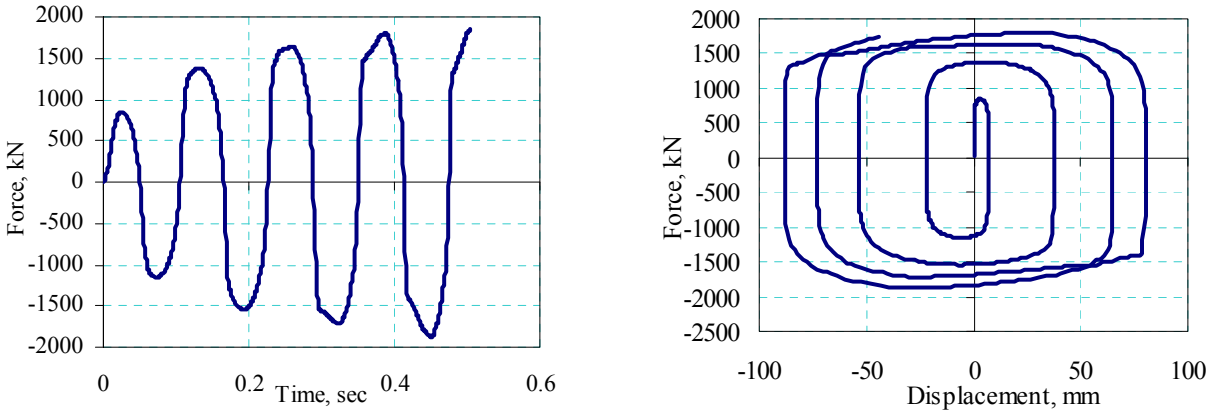

Figure 6. Force limit state simulation.

Stroke Limit States

This simulation was conducted to investigate the damper response for the limit state when the stroke limit in extension and retraction are reached. The undercut tensile and piston and driver brace compressive capacity were artificially set to be large enough for these members to remain elastic. The response is shown in Figure 7. Note that the force transmitted by the cylinder walls is non-zero, once the stoke limit in either tension or compression is reached. The total force transmitted by the damper is the sum of displacement-proportional elastic force in the cylinder wall and velocity-proportional force in the viscous component (Kelvin model). Once the stoke limit is reached, the velocity drops to zero and thus the force in the viscous element is zero. In structural applications, this will tend to translate to increased lateral stiffness and decreased effective damping ratio.

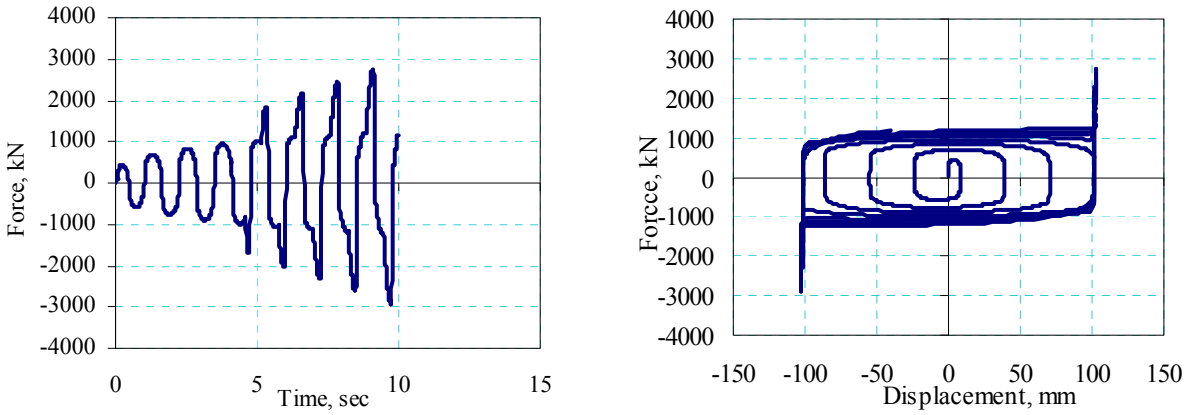

Figure 7. Displacement limit state simulation.

Compound Limit State

The stroke limit is reached first. If the loading is increased, then the driver will buckle in compression or the undercut will yield and fracture in tension. This simulation was conducted to investigate the damper response for the limit state of piston fracture following bottoming out of damper at full extension; the response is shown in Figure 8. At 4.5 sec in the response, the piston extension reaches the stroke limit and the damper bottoms out. At this point, velocity is zero and thus the force in the viscous element drops to zero; the damper now acts as an elastic brace. The undercut yields but does not fracture. Loading is then reversed. This results in the disengagement of cylinder walls, and re-loading of the viscous component. At 5.3 sec, piston bottoms out again. The damper again becomes an elastic brace. Loading is increased further resulting in fracture of undercut. The entire damper is now ineffective and removed.

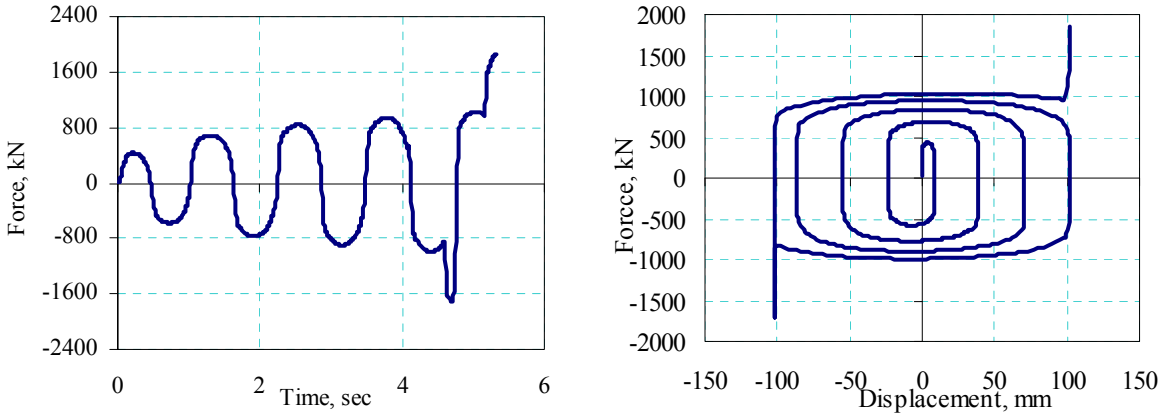

Figure 8. Compound limit state simulation.

Correlation with Test Results

Experimental data from a damper (Taylor, 2009) was used to assess the accuracy of the refined mathematical model of dampers. This damper was laboratory tested and was subjected to large velocity and displacement pulses in succession and experienced several of its limit states. This damper had a nominal capacity of 2000 kN at a velocity of 330 mm/sec. It had a stroke of

140 mm. Its constitutive relation (force in kN and velocity in mm/sec) of Eq 2.

$$F = 195\,\mathrm{sgn}(v)|v|^{0.4} \tag{2}$$

The damper was placed in the test rig and subject to a displacement loading history. The unit was placed with its piston extended to within 10 mm of the stroke limit prior to start of the displacement cycles. At 4.3 sec, the unit was pulled in tension with a large velocity pulse. The motion was reversed just prior to reaching the stroke limit. At 4.61 sec, the damper bottoms out in tension, resulting in sharp increase in the measured force. This is followed by tensile yielding. Finally at 4.68 sec, fracture occurs and the damper load drops to zero. After this time, no force can be transferred by the damper. The experimental data are presented as solid lines in Fig. 9. The dashed lines in these figures represent the results obtain from simulation using the refined damper element. Good correlation is obtained between the experimental data and analytical simulations. The analytical model was able to capture the bottoming of the damper and tensile fracture accurately.

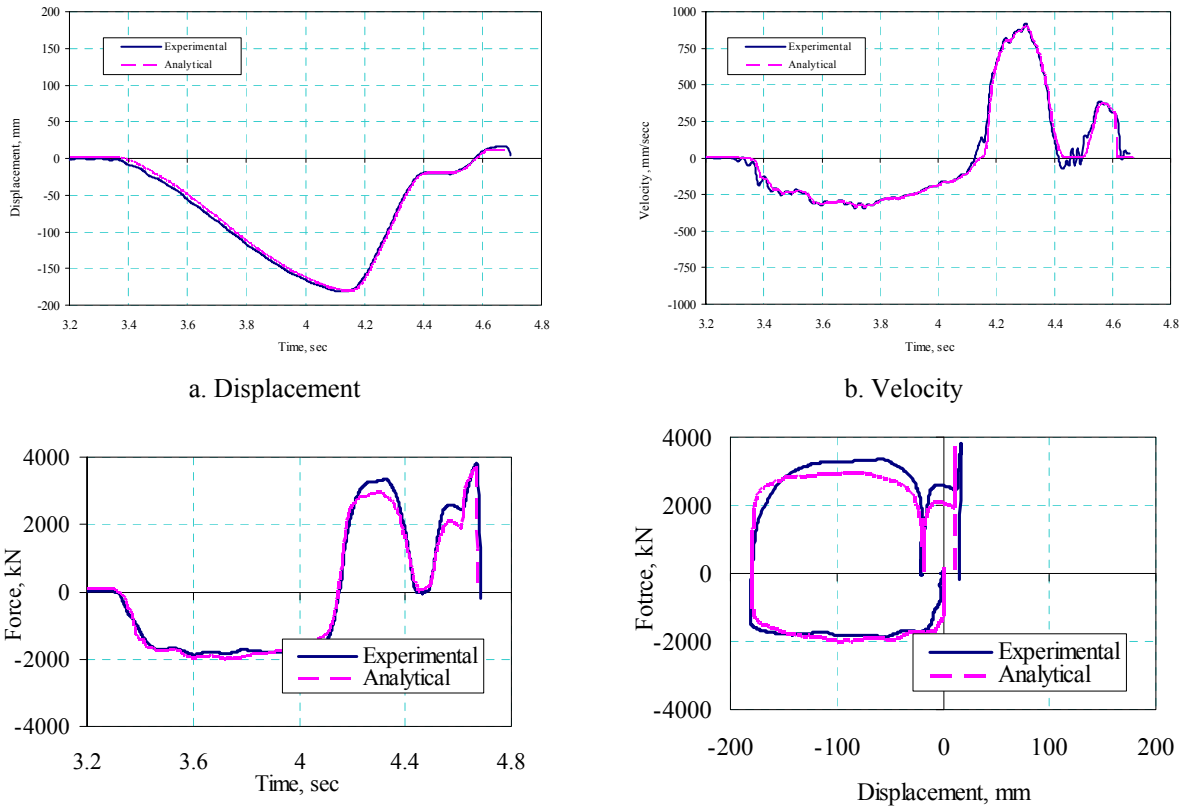

a. Displacement

b. Velocity

c. Force

d. Force-displacement hysteresis

Figure 9. Correlation with experimental data.

Nonlinear Analysis Program

The input histories used in analysis were based on the two components of the 22 far-filed (measured 10 km or more from fault rupture) pairs of NGA records (PEER 2009). These 44

records have been identified by FEMA P695 (FEMA 2009) for collapse evaluation analysis. The selected records correspond to a relatively large sample of strong recorded motions that are consistent with the code (ASCE 2005) and are structure-type and site-hazard independent. Figure 10 presents the acceleration response spectra for these records. The design MCE spectrum is shown as the dark solid line in the figure. For analysis, the 44 records were first normalized and then scaled. Normalization of the records was done to remove the record-to-record variation in intensity. Program OpenSees was used to conduct the nonlinear analyses described in this paper. Pertinent model properties are listed here.

- Analytical models are two-dimensional
- Beam and column elements, are represented as one dimensional frame elements. The members are prismatic and linear.
- Material nonlinearity is represented by concentrated plastic hinges represented by RBS hinges placed at the center of the reduced section
- The damper element is represented by the refined model including the limit states.

For collapse analysis, the normalized records are then scaled upward or downward to obtain data points for the nonlinear incremental dynamic analysis (IDA) simulations (Vamvatsikos and Cornell 2004).

One Story Moment Frame

The one-story frame is square in plan and measures 90 ft. on each side. It is 13 ft. tall (see Figure 11). The structure has one interior steel moment resisting frame on the perimeter on each side. One of the frames was selected for design and analysis. The frame was designed using the code provisions and special seismic requirements for special moment resisting frames. The ASCE/SEI 7-05 maximum period used to compute base shear (Tmax=cuTa) is 0.31 second. This period is used for scaling of ground motions as recommended by FEMA P695.

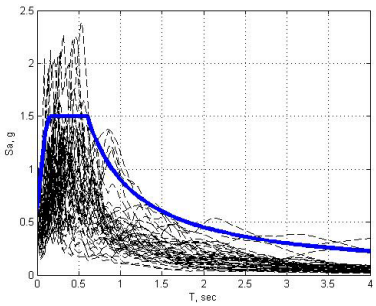

Figure 10. Response spectra of the records.

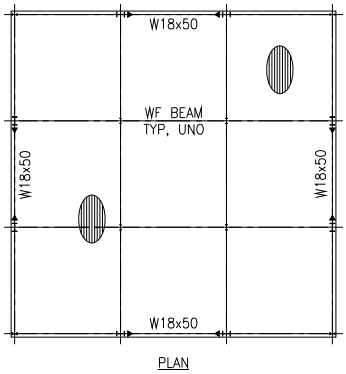

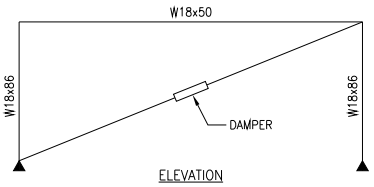

Figure 11. Views of one bay frame.

Archetypes

Five one-story archetypes were analyzed. Details for these cases are listed in Table 1. For the remainder of this paper, result from cases O-2 and O-3 are presented.

Table 1. One story archetypes

Archetype→	**O1**	**O2**	**O3**	**O4**	**O5**
Column base	Fixed	Pinned	Pinned	Fixed	Fixed
Dampers	No	Yes	Yes	Yes	Yes
Damper FS	Pinned	1.0 MCE	1.3 MCE	1.0 MCE	1.3 MCE

Pushover Analysis

Figure 12 presents the static pushover curves for archetypes O1 and O3. The pushover curves are asymmetric because the driver brace compression capacity exceeds piston undercut tensile capacity and because there is yield plateau for the buckling quadrant. Both systems are ductile with displacement ductility (μc) in excess of 8.00. The O3 archetype is superior due to the damper having a higher factor of safety.

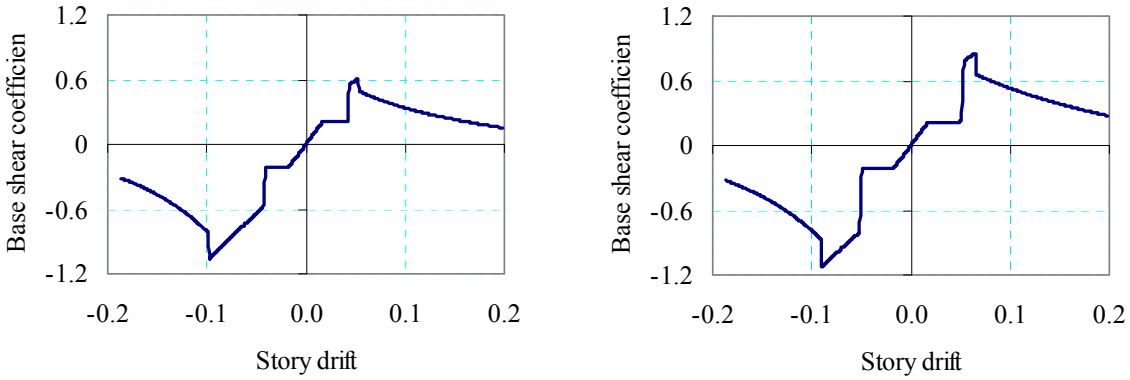

Figure 12. Pushover curves for archetypes O1 and O3

Incremental Dynamic Analysis (IDA)

Figure 13 presents the IDA plots for cases O1 and O2. The data points and the analysis trends are identified by the dashed lines and markers. The plots are shown as the scaled input spectral; acceleration (Sa) at period Tmax versus the story drift ratio.

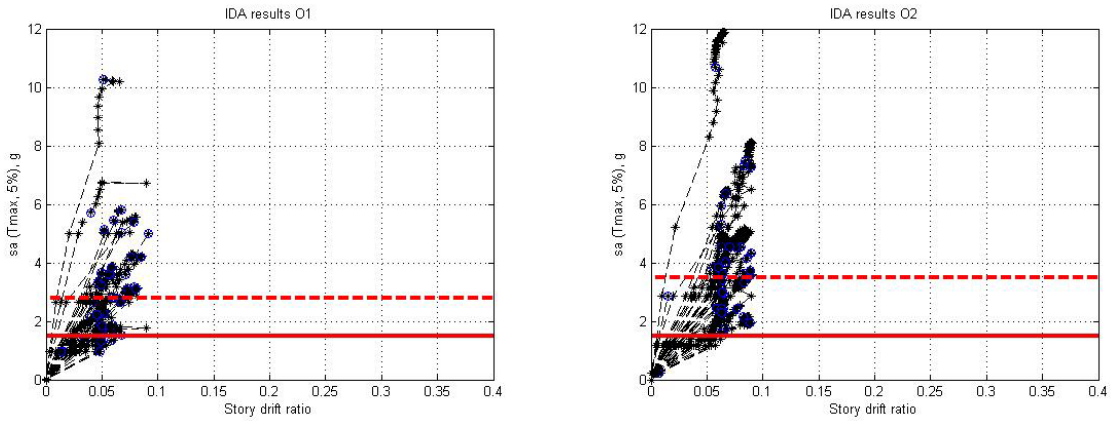

Figure 13. IDA curves for archetypes O1 and O2

The collapse point for each record was indented at the point where either the story drift ratio exceeded 0.18 or when the nonlinear tangent slope of the force-deformation curve dropped below 1% of the initial elastic slope. The median collapse Sa (SCT) is shown as the thick dashed line in the figures. The solid horizontal line is the Sa value at Tmax (SMT). The collapse margin ratio (CMR) is defined as the ratio of SCT and SMT. The adjusted collapse margin ratio (ACMR) is computed by multiplying the coefficient spectral shape factor (SSF) by the CMR. SSF depends on the building period and its ductility. Table 2 summarizes the pertinent data for the archetypes. Since the archetypes have ACMRs of greater than the ATC-63 minimum (2.02) (ATC 2009), they both pass. However, the performance of archetype O2 with a 1.3 damper factor of safety is superior.

Fragility Plots

Figure 14 presents the fragility plots for cases O-2 and O3. The data points correspond to the 44 collapse Sa values. A best-fit log-normal plot is also shown in the figure. To account for uncertainties, ATC-63 recommends a standard deviation (βTOT) of 0.55 for the case of good to excellent analysis method and available experimental data. Using this value, a revised fragility plot for each case was obtained. Using this plot, the probability of collapse at the MCE intensity is then computed. As shown in Table 2, both archetypes pass. However, the additional 30% factor of safety results in significant reduction in the collapse probability.

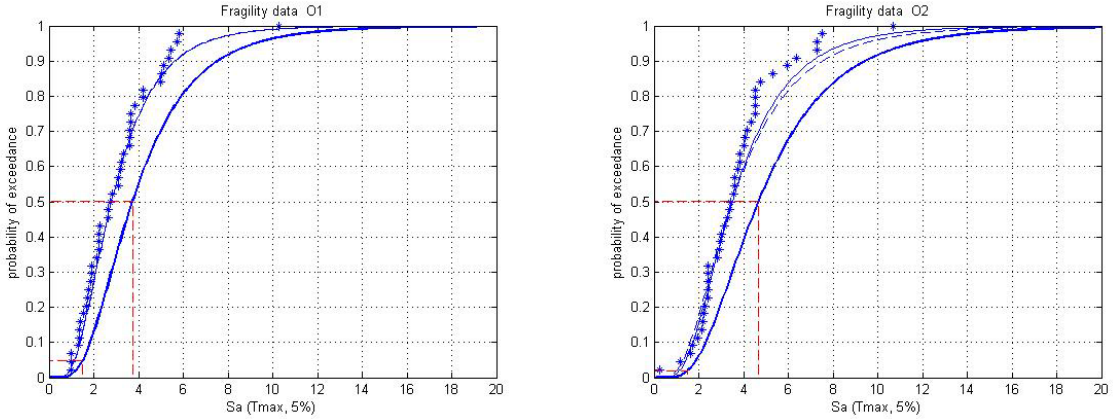

Figure 14. IDA curves for archetypes O1 and O2

Table 2. IDA results

Archetype	μc*	SSF	CMR	ACMR	$ACRM_{min}$	Pass/fail	MCE coll.	Max
O1	8.00	1.34	1.86	2.48	2.02	Pass	5%	20%
O2	8.00	1.34	2.32	3.11	2.02	Pass	2%	20%

Conclusions

Viscous dampers are added to steel moment frames structures can be used to reduce cost and improve seismic performance. IDA analysis was conducted to assess the efficacy of this methodology.

- For large earthquakes, the damper limit states must be accounted for.

- The damped structures designed per code provisions passed the ATC-63 requirements.
- Addition of a factor of safety to the damper design is cost effective and improves the performance significantly.
- For seismic upgrade, the confidence in meeting the target performance level is enhanced with the use of factor of safety in the design of viscous dampers and the resulting reduction in probability of collapse.
- A larger factor of safety would provide enhanced performance. This is especially important for retrofit application of non-ductile structures for which the loss of dampers could lead to significant damage or collapse.

Acknowledgements

Mr. Christopher Ariyaratana of University of Illinois was responsible for conducting the simulations reported in this paper. This effort is greatly appreciated. The authors acknowledge financial support from the Taylor Devices and Armor Steel. The technical assistance of Messrs. Doug Taylor and John Metzger of Taylor Devices and Dr. Kurt Haselton of California State University Chico is acknowledged.

References

American Society of Civil Engineers (ASCE), 2005. *ASCE/SEI 7-05: Minimum Design Loads for Buildings and Other Structures*, American Society of Civil Engineers, Reston, VA.

Applied Technology Council (ATC), 2009. *ATC-63 (FEMA P695): Quantification of Building System Performance and Response Parameters,* Applied Technology Center, Redwood City, CA.

Federal Emergency Management Agency (FEMA), 2008, *FEMA P695: Quantification of Building Seismic Performance Factors*, Federal Emergency Management Agency, Washington, D.C.

Miyamoto, H.K. and A. Gilani, 2008. Design of a new steel-framed building using ASCE 7 damper provisions. *Proceedings of ASCE Structures Congress*, Vancouver, BC.

Pacific Earthquake Engineering Research Center (PEER), 2009. *Open System for Earthquake Engineering Simulation (OpenSees)*, Pacific Earthquake Engineering Research Center, University of California, Berkeley. Berkeley, CA.

Pacific Earthquake Engineering Research Center (PEER), 2009, *Peer New Generation of Attenuation (NGA) Records*, Pacific Earthquake Engineering Research Center, University of California, Berkeley. Berkeley, CA.

Taylor Devices, 2009. Personal communications.

Vamvatsikos, D. and A. C. Cornell, 2004. Applied Incremental Dynamic Analysis, *Earthquake Spectra*, 20(2) 523–553, Earthquake Engineering Research Institute, Oakland, CA.